

Catalytic cracking of gas oil derived from heavy crude oil over biochar-based catalyst

Yakup Kar* & Onur Eser Kök

Iskenderun Technical University, Faculty of Engineering and Natural Sciences, Department of Petroleum and Natural Gas Engineering-31200, Hatay-Turkey

*E-mail: yakup.kar@iste.edu.tr

Received 13 October 2022; accepted 1 August 2023

In this study, the main target is to obtain high grade light commercial motor fuels from the catalytic cracking of the gas oil fraction by using a modified green catalyst biochar. For this aim, initially the biochar has been impregnated with the spent pickling liquor to acquire a catalyst being strong cracking activity under certain conditions. By using of the catalyst activated via the spent pickling liquor, the catalytic cracking runs have been carried out on the gas oil at different catalyst additive rates in ranging from 5 wt.% to 20 wt.% to obtain light liquid hydrocarbon fractions at the temperature of 500°C and heating rate of 10 °C/min. The *n*-pentane soluble fraction of the catalytic cracking liquid obtained from the use of activated char catalyst at additive rate of 20 wt.% has a low sulphur content and also consisted of short straight chain paraffinic hydrocarbons with carbon number of C₁₃, C₁₇, and C₁₈ compared to those of the thermal and non-activated catalyst. Consequently, the activated catalyst has a considerable potential as a green catalyst with low cost for the converting of heavy hydrocarbons into light and more valuable hydrocarbons.

Keywords: Biochar, Catalytic cracking, Gas oil, Green catalyst, Motor fuel

Currently, the crude oil has been still thought one of the most important energy sources in the world. It plays a key role both in increasing the level of social welfare of societies and in running of many industrial production activities. In addition, the crude oil as a commercial raw material is processed in the refineries for various high value-added products, such as petrochemicals, coke, asphalt, liquid and gaseous fuels, etc. However, the refinerable oil (conventional crude oil) reserves are alarmingly decreasing day by day due to an incredible increase in its global consumption. In order to meet demand in this area, the exploitation of the heavy oil resources found in high reserves; which is equal to at least 25% of total crude oil reserves in the world¹, has been attracting researchers in the recent years.

Heavy oil is commonly defined as the unconventional oil of a specific gravity of API ≤ 20° (Ref. 2). It has extremely high viscosity and a molecular structure with a great amount of S, O and N, which lead to occurrence of some challenges during its exploitation, transportation and processing³. To avoid these difficulties, the reduction of its viscosity and heteroatom content by running suitable low-cost improvement techniques is very important. Among the

applied current techniques with this aim, one of the most popular ones is catalytic cracking. By means of this process, the large hydrocarbon molecules of a heavy distillate like gas oil can be successfully converted into the smaller ones which took place in the high value-added light end products such as diesel, gasoline and LPG⁴. Catalytic cracking of heavy hydrocarbons is achieved at certain process conditions and also the presence of suitable catalyst. However, the cracking catalysts used in modern refineries are quite costly. Therefore, there is a crucial importance that the creation of new catalysts with low-cost to be used for this aim in order to reduce the high cost burden resulted from the catalyst. With this aim, nowadays a lot of studies are being done on the functionalization of various biochar-based catalysts with various techniques^{5,6}. Recently, a review on biochar-based catalysts was reported by Xiong et al.⁷, which emphasized that the catalytic performances of the biochar-based catalysts were better compared to those of the conventional catalysts derived from silica, resin, or carbon. Shen et al.⁸ studied the catalytic conversion of tar using the rice husk char-supported Ni and Fe catalysts. End of this study, they obtained high tar conversion yield of about 93%. In one other study, it

was stated that the bio-oil upgraded with using Ni supported-biochar catalyst was rich in hydrocarbon content (approximately 80%) due to the high activity and selectivity of the catalyst. The authors stated also in this study that the upgraded product has rich content in terms of n-heptadecane which is a very important constituent of diesel fuel⁹. In addition, it was reported in another study that the high catalytic conversion efficiency of bio-syngas into liquid hydrocarbons was achieved on biochar-based iron catalyst and this situation was attributed to the strong interaction of metal-carbon between the biochar and the supported metals¹⁰. On the other hand, a biochar not activated with physical or various chemical agents has poor catalytic effectiveness⁵. To deal with this situation, the biochar can be activated with applying a suitable activation method such as chemical treatment, gas activation, and metal impregnation⁷. The activation applied results in the occurrence of significant changes in the surface morphology and surface functionality of biochar being effective on for using of it as a catalyst⁶. By means of the metal impregnation, especially with loading of various active metals such as iron and nickel into biochar, a higher catalytic activity can be achieved^{11,12}. Based on all of these literatures, as stated by Cheng and Li¹¹, the biochar-based catalysts can be considered as an alternative option for the traditional ones with high cost and non-renewable.

In view of the relevant literatures, the main target of the present study is to create a new biochar-based catalyst with low-cost and high catalytic cracking efficiency. Then, the catalytic cracking efficiency of the obtained biochar-based catalyst on the conversion of gas oil fraction derived from a heavy crude oil into light end products such as gasoline, kerosene, and diesel, etc. is to be tested under certain process conditions. The obtained end products were characterized according to the ASTM standards.

The most important part of our study is use of two by-product materials (biochar as main feedstock and spent pickling liquor as metal precursor) in designing the catalyst. Furthermore, the spent pickling liquor (SPL) which is a waste product of iron and steel industry was firstly evaluated as metal precursor by our group and used in this study to prepare biochar-based catalyst.

Experimental Section

Materials

The gas oil fraction and biochar as main raw feedstocks for designing our catalyst were obtained

from our earlier experiments. The biochar which is a solid by-product of ~27wt.% of yield was derived from the pyrolysis of almond shell of biomass at 500°C and 10 °C/min¹³. The gas oil fraction with a yield of ~31wt.% is a distillate fraction with boiling point range of 290-360°C of Bati Raman heavy crude oil pretreated¹⁴. The SPL as a metal precursor was supplied by the İskenderun Tosçelik Factory. The results of chemical analysis of the SPL are presented in Table 1.

Preparation of biochar-based catalysts

The catalysts of biochar-based were prepared by impregnation method. For this purpose, approximately 35 g of biochar and 350 mL of SPL were loaded in a glass reactor of 500 mL capacity and the mixture was heated on a magnetic stirring heater under a reflux condenser at 110°C for 4 h. After the treatment of the SPL, the soaked char sample was filtered to remove the remaining of SPL with aim of a funnel filtering apparatus, and then was washed four times with pure water. The washed activated biochar was dried in an oven at 110°C for 12 h. The dried biochar catalysts were named as C1 (activated without the SPL) and C2 (activated with SPL). Lastly, the activated biochars were bottled for further studies.

Characterization of the prepared catalysts

In order to evaluate the effect of the SPL agent on the biochar catalyst, the surface morphology, elemental contents and thermal degradation behaviour of the biochar catalysts were determined via CHNS (Thermo Scientific Flash 2000), FT-IR (FTIR-IR-Affinity, SHIMADZU) and SEM (JEOL 5500/OXFORD Inca-X) analyses.

Catalytic cracking of gas oil with biochar-based catalysts

The gas oil fraction was cracked in a fixed-bed reactor detailed in the earlier study¹³ under certain cracking conditions of temperature 500°C and heating

Table 1 — Chemical analysis results of the spent pickling liquor

Parameter	(mg/L)	Parameter	(mg/L)
Mn	573.2872	Cr	59.9203
P	316.5836	Cu	24.4757
Zn	19804.6918	Ti	1.1583
Pb	8.4016	Ca	82.3734
S	75.4648	Mg	51.5198
Si	0.0000	K	20.0562
Al	79.9589	Ba	1.3962
Ni	31.3198	Na	64.9965
	(%)		(%)
Fe	12.6100	HCl-free	3.86

rate 10°C/min. The cracking studies were carried out by using the catalysts of C1 and C2. For each cracking run, approximately 25 g of gas oil and a certain quantity of catalyst at different ratios of 5-25 wt.% were added into the fixed-bed reactor. The inside of loaded-reactor was swept by nitrogen gas for the supplying of inert atmospheric medium. Then, the mixture of gas oil and catalyst was cracked at 500°C and 10°C/min for 60 min. End of each cracking run, the cracked liquid product condensed was collected in the trap and weighed. Each of the different cracking experiments was at least repeated three times at the same conditions.

Effect of the amount of char catalysts on the yields of products

Initially, the thermal cracking of the gas oil was carried out at certain experimental conditions and the achieved yields were determined as 85.25 wt.% for the liquid, 4.07 wt.% for the solid product, and 10.68 wt.% for the gas. Following this, in order to judge the effect of the amount of the char catalysts on the product yields the individual catalytic cracking runs were executed at the same experimental conditions by using different amounts of the catalysts in ranging from 5 to 20 wt.%. The obtained yield results for the C1 and C2 catalyst are given in Fig. 1a and Fig. 1b, respectively.

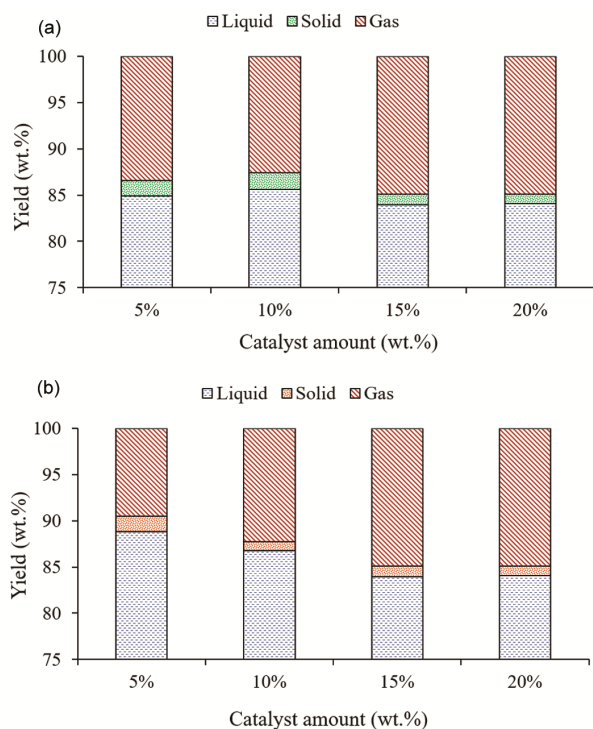


Fig. 1 — Effect of amount of (a) C2 and (b) C1 char catalyst on the product yields

By increasing the C1 char catalyst amount from 5 wt.% to 20 wt.%; while the liquid yield receded from 88.83 wt.% to 86.09 wt.%, the solid yield diminished from 1.64 wt.% to 1.33 wt.% harmoniously. On the contrary to the observed decreases in the yields of the liquid and solid, for the same catalyst amounts the gas yield increased from 9.53 wt.% to 12.58 wt.% with a significant increase. As for the catalytic cracking results of the C2 char catalyst, the liquid yield diminished from 84.88 wt.% for 5.0 wt.% of the catalyst to 84.09 wt.% for 20 wt.% of it with a slight reduction. Yet, for the same catalyst amount the more decrease in the solid yield was happened with decreasing the catalyst amount from 1.68 wt.% to 1.00 wt.%. On the other hand, the obtained gas yields for the used catalyst amounts were 13.44 wt.% and 14.91 wt.%, respectively. When compared these yields, the decreases in the liquid and solid yields leading to the rise in the gas yield may be connected with the catalytic cracking effect of the used catalysts in this study. Moreover, from the use of the C2 char catalyst with 20 wt.%; the catalytic cracking yields resulted in as 84.09 wt.% (liquid), 1.00 wt.% (solid), and 14.91 wt.% (gas). As seen in the yields, the catalytic yields belonging to the liquid and solid product were in lower levels compared to that of the thermal cracking and also that of the catalytic cracking requiring the use of the C1 char catalyst with the same amount. However, the gas yield for the C2 catalyst with 20 wt.% amount was higher compared to those of the others as expected. That shift in the yields can be attributed to the stronger catalytic cracking influence of the C2 char catalyst on heavy hydrocarbons triggered by the active sites like Fe loaded on it. Additionally, this interpretation was in largely harmonious with the studies reported previously^{8,15,16,17}.

Characterization of the cracking liquid products

The light oils of the catalytic cracking of gas oil were analyzed for some of their physicochemical properties such as hydrocarbon distributions, viscosity, H/C ratio, HHV, etc. In order to determine the hydrocarbon distributions of the oils, the gas chromatography-mass spectrometry (GC-MS) analysis were performed on the HP 6890 GC analyzer with an HP 5973 MSD detector via an HP-Innowax column (60 m×0.25 mm×0.25 μm) according to the detailed method¹⁸. The kinematic viscosities of the obtained catalytic liquids were analyzed according to the ASTM D 446.

Results and Discussion

Characterization of the prepared biochar catalysts

While the carbon content value of 76.57 wt.% for the catalyst C1 was lower than 77.24 wt.% of the catalyst C2, the values of H, N, and O determined as 3.02 wt.%, 1.25 wt.%, and 19.17 wt.%, respectively, for the catalyst C1 were higher than those (2.88 wt.% H, 1.18 wt.% N, and 18.70 wt.% O) of the catalyst C2. Based on these data, it can be said that the activating process led to slightly increase in the percentage of C while leading to some decrease in the H, N, and O values. These changes in the elemental contents of the biochars may be linked to the textural structure of the biochar which interacts with the metal species in the SPL agent. The similar situation was stated for the C and O contents of the magnetic and non-magnetic biochars¹⁹.

To identify the surface functional groups of the raw biochar of C1 and activated biochar of C2, the FT-IR tests were conducted on the biochars of C1 and C2 and the obtained spectra are illustrated in Fig. 2. From the FT-IR spectra, it is clearly seen that many known biochar surface functional groups^{5,6,20} with different intensities were recorded for the biochars of C1 and C2 owing to interacting of the functional groups of C1 with the metal species in the SPL agent. This situation was in agreement with the result that the iron-impregnation process altered the surface functional groups of biochar^{21,22}. The peaks at 1577.49 cm⁻¹ and 1578.45 cm⁻¹ respectively, for biochar of C1 and C2 may be attributed to the functional group of C=O stretching reported for the peak around 1577 cm⁻¹. Compared with C1 spectrum, the peaks at 2985.27 cm⁻¹ and 2900.41 cm⁻¹ were only appeared for the biochar of C2 and these peaks might correspond to the stretching vibration of C-H. The peaks at 1061.62 cm⁻¹ and 1245.79 cm⁻¹ for the biochar of C2 besides those at 1021.12 cm⁻¹ and

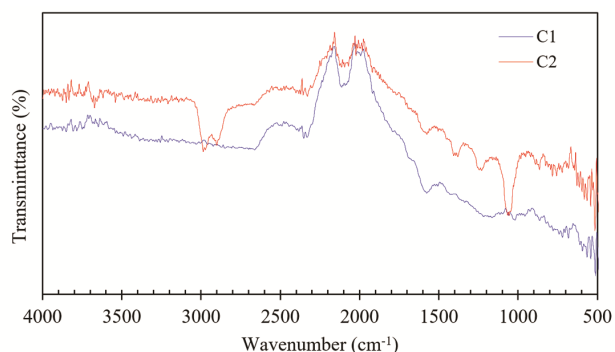


Fig. 2 — FT-IR spectra of the biochar of C1 and C2

1218.79 cm⁻¹ belonging to the biochar of C1 between 1000-1300 cm⁻¹ could be attributed to the C-O bending vibration²³. The peaks at 1418.39 and 1406.82 cm⁻¹ for the biochars of C1 and C2, respectively, may be assigned to the C = C stretching vibration. For both chars, the peaks ranging from 3400 cm⁻¹ to 3875 cm⁻¹ might be attributed to the N-H stretching and -OH group modes. For the biochar of C2, the peak seen at 582.40 cm⁻¹ could be attributed to the presence of Fe-O stretching vibration bonds²⁴. Additionally, the stated peak of Fe-O for this study was imminently consistent with those of others^{19,25,26}.

The SEM images of the biochars (C1 and C2) are shown in Fig. 3. A number of pores and hollows with different size and shapes are observed at the surface of biochars. From Fig. 3, it is clearly seen that the surface morphology of the biochar of C1 has both more regular-well developed pore structure and smooth surface as compared to that of C2. These differences related to the surface-morphology can be attributed to the interaction of the metal species with the fine pore of the biochar of C1.

Characterization of the cracking liquid products

First, about 2 g of each cracking liquid (C1-0, C1-20, and C2-20) was sorted into two main fractions as *n*-pentane soluble and insoluble by using 100 mL of *n*-pentane solvent. The yields of the *n*-pentane soluble fraction were approximately 93.81 wt.% for the C1-0, 91.47 wt.% for the C1-20, and 94.53 wt.% for the C2-20 respectively. These results indicated that the yield of 94.53 wt. for the C2-20 was higher than those of the others. This higher *n*-pentane soluble yield for the C2-20 compared to the others may attributed to the possible-strong catalytic cracking effect of the C2 catalyst on some gas oil components with long chain and high carbon number.

For detailed assessment regarding the catalytic effect, the GC-MS analysis of the *n*-pentane soluble fractions of C1-0, C1-20 and C2-20 was executed according to the analysis method detailed in the previous study¹⁸. The GC-MS analysis results were given in Table 2. As seen in Table 2, the analyzed fractions included primarily *n*-paraffins, olefins and benzothiophenes in different concentrations (as area%). The C1-0 fraction hold the paraffins of 57.38% (as total area%), olefins of 1.48 %, and 22.74% of benzothiophenes, respectively. For the C1-20, the chemical content values were happened as 33.25% of paraffins, 5.10% of olefins, and 20.44% of

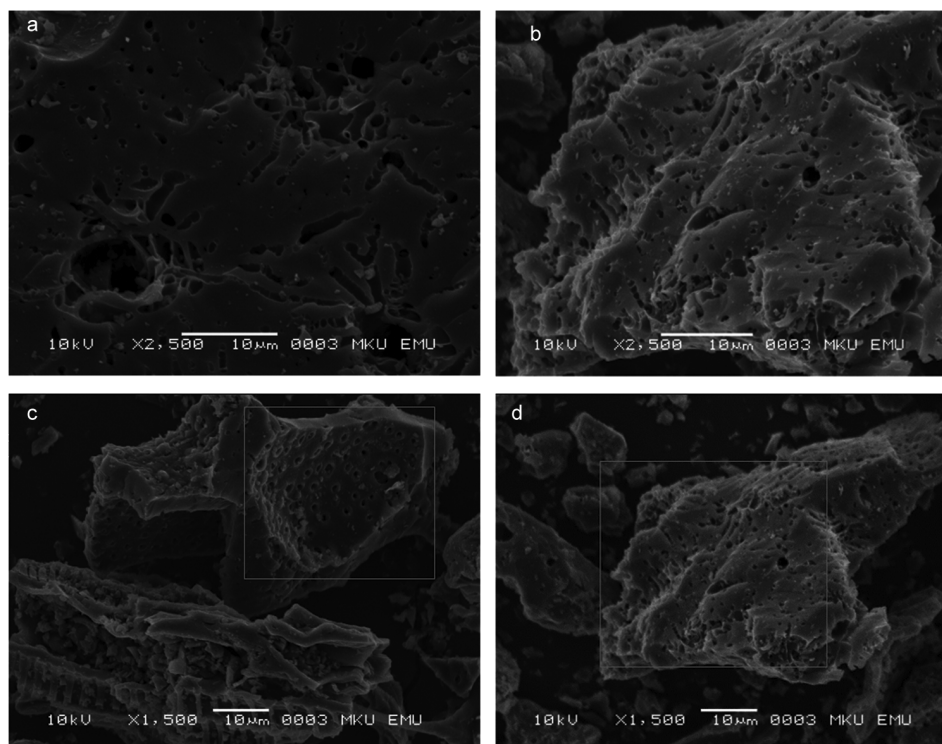


Fig. 3 — The SEM images for the biochar of (a) C1 and (b) C2

Table 2 — GC-MS analysis results of the *n*-pentane soluble fractions of the cracking products (C1-0, C1-20 and C2-20)

Name of compound	Formula	RT (min)	C1-0 PA (%)	C1-20 PA (%)	C2-20 PA (%)
1-Decene	C ₁₀ H ₂₀	6.219	nd	nd	0.20
Tridecane	C ₁₃ H ₂₈	17.835	nd	0.53	1.10
Pentadecane	C ₁₅ H ₃₂	24.490	0.51	2.47	1.32
Hexadecane	C ₁₆ H ₃₄	27.042	6.17	nd	3.84
Heptadecane	C ₁₇ H ₃₆	29.502	3.11	4.45	4.52
1-Nonadecene	C ₁₉ H ₃₈	30.538	1.48	5.10	2.97
Octadecane	C ₁₈ H ₃₈	32.535	nd	2.94	3.03
Nonadecane	C ₁₉ H ₄₀	36.517	1.50	2.44	nd
Benzo[b]thiophene, 3,6-dimethyl-	C ₁₀ H ₁₀ S	38.709	1.24	2.10	nd
Eicosane	C ₂₀ H ₄₂	42.148	9.23	9.62	5.65
Benzo[b]thiophene, 2,5,7-trimethyl-	C ₁₁ H ₁₂ S	45.913	nd	0.94	nd
Heneicosane	C ₂₁ H ₄₄	50.330	2.59	nd	nd
Tricosane	C ₂₃ H ₄₈	58.947	12.40	10.80	6.89
Pentacosane	C ₂₅ H ₅₂	63.754	10.63	nd	nd
Hexacosane	C ₂₆ H ₅₄	65.642	11.24	nd	nd
Dibenzothiophene, 4-methyl-	C ₁₃ H ₁₀ S	67.336	21.50	7.67	13.25
Dibenzothiophene, 3-methyl-	C ₁₃ H ₁₀ S	68.606	nd	9.73	nd

RT: Retention time, PA: Peak area, nd: not detected

benzothiophenes. Lastly, these data were established for the C2-20 fraction as 26.35%, 3.17%, and 15.31%, respectively. Based on these results, it could be stated that all fractions were rich in paraffinic content.

Additionally, that situation has been confirmed by the FT-IR spectra (see Fig 4.) for the all liquids. As seen in the Fig. 4, the saturated C-H stretching vibration peaks of 3000-2800 cm⁻¹ and the C-H bending

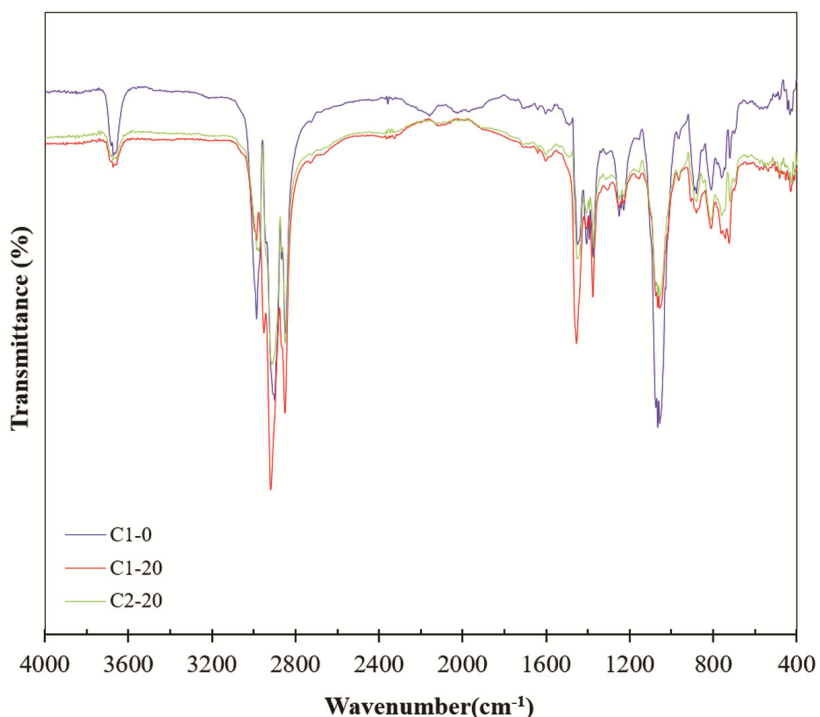


Fig. 4 — FT-IR spectra of the cracking liquid products

vibration peaks of $1300\text{--}1500\text{ cm}^{-1}$ show the presence of alkane compounds in the liquid products²⁷. On the other hands, the occurrence of the peaks in the region less than 1500 cm^{-1} can be ascribed to the presence of the benzothiophenes²⁸. As an indicator for the alkenes, the peaks resulting from the unsaturated C-H out-of-plane bending vibrations between 1000 and 650 cm^{-1} ²⁷ can be indicated. Consequently, the FT-IR results are in line with the GC-MS results.

To assess the cracking effect of the C1 and C2 catalyst on the paraffinic hydrocarbon distributions of the C1-0, C1-20, and C2-20 liquid products, the calculated concentration values (peak area %) of the detected straight chain alkanes was presented based on their carbon numbers as shown in Fig 5. According to these carbon distributions, the liquid of C1-0 consists of the paraffinic compounds with C₁₅–C₁₇, C₁₉–C₂₁, C₂₃, C₂₅, and C₂₆ carbon number. On the other hand, while the C1-20 liquid possesses the n-alkanes with C₁₃, C₁₅, C₁₇–C₂₀, and C₂₃ carbon number, the C2-20 liquid includes the n-alkanes with C₁₃, C₁₅–C₁₈, C₂₀, and C₂₃ carbon number. These results indicate that the C2-20 catalytic liquid did not include the long chain compounds with C₂₅ and C₂₆ carbon number compared to the C1-0 liquid. Furthermore, the C2-20 liquid consisted of important paraffinic compounds with low carbon number is in agreement

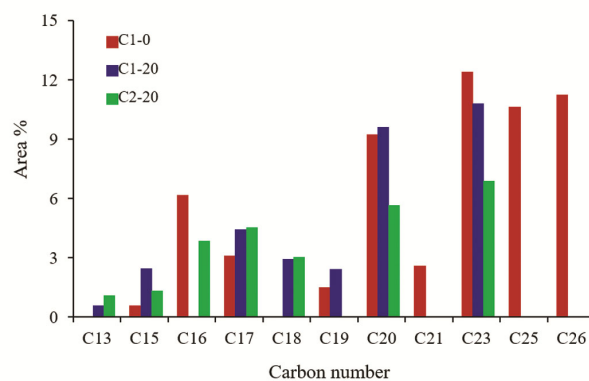


Fig. 5 — Carbon number distribution of the paraffins of the *n*-pentane soluble fractions

with the C₁₃–C₂₂ carbon number range of the diesel fuel²⁹. In addition to this, the C2-20 liquid had higher content than the others in view of the shorter chain compounds with C₁₃, C₁₇, and C₁₈ carbon number. This case can be attributed to the strong catalytic cracking activity of the C2-20 catalyst over the long chain hydrocarbon molecules of the gas oil. The strong catalytic cracking effect of the C2-20 catalyst can be connected with the presence of the metallic species like Fe loaded onto the char via the activating solution^{8,17,30} (see Table 1).

Table 3 — Elemental analysis results of the *n*-pentane soluble fractions

Sample	%C	%H	%N	%S	%O ^a	(H/C) ^c	(O/C) ^c	HHV ^b (MJ/kg)
C1-0	82.40	11.54	0.017	4.428	1.615	1.669	0.015	42.64
C1-20	82.81	11.33	0.027	4.337	1.496	1.630	0.014	42.54
C2-20	82.69	11.28	0.025	4.277	1.728	1.626	0.016	42.41

^a From the difference

^b Calculated via the formula

^c Molar ratio

For further assessment, the elemental analyses of the *n*-pentane soluble fractions of the liquid products were executed and the obtained analysis results and the higher heating values (HHVs) were presented in Table 3. According to these results, we could explicitly declare that the catalytic cracking liquid products (C1-20 and C2-20) were of lower sulphur content than the thermal cracking liquid (C1-0). Furthermore, the C2-20 liquid had the lower sulphur content than the others. Its lower sulphur content can be linked to the enhancing effect of the Fe dispersed finely on the C2 char catalyst on the C-S bond breaking activity resulting in a decrease in the amounts of sulphur species thiophenic compounds such benzothiophenes (BTs) and dibenzothiophenes (DBTs)³⁰. These elemental sulphur content values in Table 3 are completely in harmony with the concentration values of sulphur species (see Table 2). At the same time, the obtaining liquid product with lower sulfur content from catalytic cracking of gas oil was in line with the related literature⁴. Consequently, the C2 char catalyst enjoys the usage potential for the desulphurization and catalytic cracking processes of various heavy oil fractions like gas oil etc.

In order to evaluate the use potential of the obtained liquid products as a suitable transportation fuel, the H/C (molar ratio) values were calculated from their elemental analysis results and the obtained values were given in Table 3. As can be observed from Table 3, The H/C ratios were approximately in the range of 1.67-1.63 for the cracking oils. These ratio values are in compatible with the raw diesel ratio of 1.65 (Ref. 31). A high heating value of a potential fuel is generally considered as an important indicator to achieve the high thermal efficiency and power output³². In this context, the higher heating values (HHVs) of the obtained cracking oils were calculated from the equation³³ with running the elemental analysis results. The HHVs values of the cracking oils in range of 42.41- 42.64 MJ/kg were almost equal to 42.7 MJ/kg of the conventional diesel³⁴. Apart from the HHVs, to judge the quality of a fuel the other

critical physical property is kinematic viscosity. The kinematic viscosity values of the catalytic cracking liquids were determined as 4.33 cSt (40°C) for the C2-20 and 5.55 cSt (40°C) for the C1-20 liquid. As a result, the viscosity of the C2-20 liquid product was determined as lower in compared with that of the C1-20 due to its high light content consisting of low molecular weight *n*-paraffinic compounds. The viscosity value of 4.33 cSt for the catalytic liquid product was also in agreement with that of the automotive diesel fuel in the range of 2.0-4.5 at 40°C³⁵. Consequently, all the obtained results reveals that the C2 char can be exploited as the low-cost cracking catalyst to achieve the light fractions with lower sulphur content from the catalytic cracking of petroleum heavy fractions such as gas oil, etc.

Conclusion

This study was mainly implemented to obtain light fractions from the conversion of the gas oil fraction via the thermal and also catalytic cracking processes. So as to achieve that, the catalytic cracking runs were executed on it by usage of the catalysts-based on the biomass chars either impregnated with the spent pickling liquor with rich iron content (named as C2 char catalyst) or to be not impregnated (called as C1 char catalyst). The obtained liquids were characterized in detailed. The spent pickling liquor altered considerably the surface morphology of biochar resulted in the C2 char catalyst. The C2-20 liquid obtained from the catalytic cracking by using the C2 char catalyst comprised of high amounts of the straight short chain paraffinic compounds with the carbon number of C₁₃, C₁₇ and C₁₈ as compared to those of the others. Additionally, The C2-20 liquid had lower viscosity that the C1-20 liquid due to a probable enhancing effect of the spent pickling liquor on catalytic cracking. The *n*-pentane soluble fraction of the C2-20 liquid had the lower thiophene molecule content, leading to the occurrence of lower sulphur content in it. As a final conclusion, it could be stated that the C2-20 char catalyst had a considerable

potential as green low cost cracking catalyst in terms of the conversion heavy carbon stocks such as gas oil into various hydrocarbon fractions with light and low sulfur contents.

References

- 1 Muraza O & Galadima A, *Fuel*, 157 (2015) 219.
- 2 Chen Q, Zhu Y, Wang M, Ren G, Liu Q, Xu Z & Sun D, *Colloids Surf A*, 560 (2019) 252.
- 3 Chao K, Chen Y, Li J, Zhang X & Dong B, *Fuel Process Technol*, 104 (2012) 174.
- 4 Da Silva A S V, Weinschutz R, Yamamoto C I & Jr Luz L F, *Fuel*, 106 (2013) 632.
- 5 Lee J, Kim K H & Kwon EE, *Renewable Sustainable Energy Rev*, 77 (2017) 70.
- 6 Qian K, Kumar A, Zhang H, Bellmer D & Huhnke R, *Renewable Sustainable Energy Rev*, 42 (2015) 1055.
- 7 Xiong X, Yu IKM, Cao L, Tsang D C W, Zhang S & Ok Y S, *Bioresource Technol*, 246 (2017) 254.
- 8 Shen Y, Zhao P, Shao Q, Ma D, Takahashi F & Yoshikawa K, *Applied Catal B*, 152 (2014) 140.
- 9 Nguyen H K, Pham V V & Do H T, *Catal Lett*, 146 (2016) 2381.
- 10 Yan Q, Wan C, Liu J, Gao J, Yu F, Zhang J & Cai Z, *Green Chem*, 15 (2013) 1631.
- 11 Cheng F & Li X, *Catalysts*, 8 (2018) 346.
- 12 Duman G & Yanık J, *Internat J Hydrogen Energy*, 42 (2017) 17000.
- 13 Kar Y, *Biomass and Bioenergy*, 119 (2018) 473.
- 14 ŞenelGöksu D & Kar Y, *Energy Sources Part A: Recovery, Utilization and Environmental Effects*, 40 (2018) 2678.
- 15 Wang S, Shan R, Gu J, Zhang J, Yuan H & Chen Y, *Fuel*, 279 (2020) 118494.
- 16 Dai L, Zeng Z, Tian X, Jiang L, Yu Z, Wu Q, Wang Y, Liu Y & Ruan R, *J Anal Appl Pyrolysis*, 143 (2019) 104691.
- 17 Lin B, Huang Q, Yang Y & Chi Y, *J Anal Appl Pyrolysis*, 139 (2019) 308.
- 18 Kar Y, *Energy Sources Part A: Recovery, Utilization, and Environmental Effects*, 40 (2018) 2812.
- 19 Son E B, Poo K M, Chang J S & Chae K J, *Science of the Total Environment*, 615 (2018) 161.
- 20 Ahmed M B, Zhou J L, Ngo H H, Guo W & Chen M, *Bioresource Technol*, 214 (2016) 836.
- 21 He R, Peng Z, Lyu H, Huang H, Nan Q & Tang J, *Science of the Total Environment*, 612 (2018) 1177.
- 22 Hu X, Ding Z, Zimmerman A R, Wang S & Gao B. *Water Research*, 68 (2015) 206.
- 23 Lu P, Huang Q, Chi Y & Yan J, *J Anal Appl Pyrolysis*, 127 (2017) 47.
- 24 Zhou X, Zhou J, Liu Y, Guo J, Ren J & Zhou F, *Fuel*, 233 (2018) 469.
- 25 Yang K, Peng H, Wen Y & Li N, *Appl Surf Sci*, 256 (2010) 3093.
- 26 Chen B, Chen Z & Lv S, *Bioresource Technol*, 102 (2011) 716.
- 27 Zhou L, Yang H, Wu H, Wang M & Cheng D, *Fuel Process Technol*, 106 (2013) 385.
- 28 Shamsace B H, Mehri F, Rowshanzamir S, Ghamati M & Behrouzifar A, *Sep Purif Technol*, 212 (2019) 505.
- 29 Aguado J, Serrano D P, San Miguel G, Castro M C & Madrid S, *J Anal Appl Pyrolysis*, 79 (2007) 415.
- 30 Muenpol S & Jitkarnka S, *J Anal Appl Pyrolysis*, 117 (2016) 147.
- 31 Hughey C A, Hendrickson C L, Rodgers R P & Marshall A G. *Energy Fuels*, 15 (2001) 1186.
- 32 Solak A & Rutkowski P, *Waste Management*, 34 (2014) 504.
- 33 Zhang Z, Chang H, Gao T, Lan T, Zhang J, Sun M, Xu L & Ma X, *J Anal Appl Pyrolysis*, 139 (2019) 31.
- 34 Ayanoğlu A & Yumrutaş R, *Energy*, 103 (2016) 456.
- 35 Vempatapu B P, Tripathi D, Kumar J & Kanaujia P K, *SN Appl Sci*, 1 (2019) 1.